Korean J. Chem. Eng., **26**(3), 828-832 (2009)

Two phase (air-molten carbonate salt) flow characteristics in a molten salt oxidation reactor

Yung-Zun Cho*,†, Hee-Chul Yang*, and Yong Kang**

*Nuclear Fuel Cycle R&D Group, Korea Atomic Energy Research Institute, Dukjin 150, Yuseong, Daejeon 305-353, Korea
**Department of Chemical Engineering, Chungnam National University, Gung 220, Yuseong, Deajeon 305-764, Korea
(*Received 10 July 2008 • accepted 3 November 2008*)

Abstract−Molten salt oxidation process is one of the most promising alternatives to incineration that can be used to effectively destroy the organic components of mixed and hazardous wastes. To detect the flow characteristics of the molten salt oxidation process (air-molten carbonate salt two-phase flow), differential pressure fluctuation signals from a molten salt oxidation process have been analyzed by adopting the stochastic methods. Effects of the input air flow rate (0.05-0.22 m/sec) and the molten salt temperature (870-970 ºC) on the phase holdup and flow characteristics are studied. The gas holdup increases with an increasing molten salt temperature due to the decrease of the viscosity and surface tension of the molten carbonate salt. It is found that a stochastic analysis of the differential pressure signals enables us to obtain the flow characteristics in the molten salt oxidation process. The experimentally obtained gas holdup data in the molten salt reactor were well described and characterized by means of the drift-flux model.

Key words: Molten Salt Reactor, Gas Holdup, Stochastic Analysis, Flow Characteristics

INTRODUCTION

Gas-liquid two phase flow system such as bubble columns have frequently functioned as gas-liquid reactors or contactors because of their simplicity, high efficiency for a gas-liquid contract, and low operating cost [1-3].

Recently, a molten salt oxidation process has been studied for the destruction of a difficult-to-treat waste. Molten salt oxidation is one of the most promising alternatives to incineration that can be used to oxidatively and efficiently destroy the organic components of mixed and hazardous wastes [4,5]. Molten salt oxidation was developed by RockWell International as a coal gasification tool, and now a days has been used for the destruction (or oxidation) of mixed wastes, chemical warfare agents, medical wastes and energetic materials such as explosives and propellants. The basic concept of a molten salt oxidation is to (1) introduce wastes and air into a molten salt bed, (2) oxidize the organic wastes in the molten salt bed, (3) retain the inorganics in the molten salt, and (4) remove the salt for a disposal or for a processing and recycling [6]. The organic components of the wastes are converted into CO_2 and H_2O through the combined effects of a pyrolysis and a oxidation. The molten salt functions as a catalyst for the conversion of the organic compounds to CO_2 and H_2O. Reactive species such as halogens and sulfur in the organic waste are converted into acid gas then it reacts with the molten salt to form the corresponding neutralized salts. Other inorganic components in the wastes are retained in the molten salt bed either as metals or as oxides [7,8].

For the proper design, scale-up and operation of a molten salt oxidation process, knowledge on the hydrodynamics is essential because these hydrodynamics strongly affect the oxidation efficiency of the molten salt oxidation process. However, there has been little attention paid to an air-molten salt two-phase flow system until now, even on the basic hydrodynamics. One of the most important hydrodynamic parameters for the proper design of a molten salt oxidation process is the gas holdup. It can directly affect the operation efficiency. Thus, in this present study, the effects of the gas velocity and the temperature on the gas phase holdup have been investigated. Furthermore, the differential pressure fluctuations have been measured and analyzed by means of a spectral analysis to describe the flow characteristics with a variation of the operating conditions.

EXPERIMENTAL

Experiments were carried out in a cylindrical column of 0.076 m

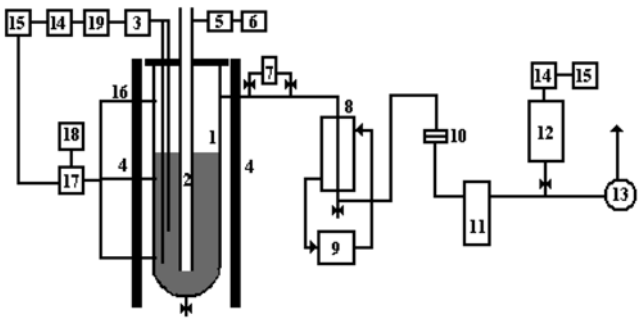

Fig. 1. Schematic diagram of the integrated molten salt oxidation system.

1. Molten salt vessel	10. HEFA filter
2. Gas/Waste injector	11. Silica bed
3. Differential pressure transducer	12. Off gas analyzer
4. Electric heater	13. I.D. fan
5. Screw feeder	14. A/D converter
6. RPM controller	15. Computer
7. Impactor	16. Thermocouple
8. Heat exchanger	17. Temperature indigater
9. Cold water bath	18. Temperature controller
	19. Low pass filter

†To whom correspondence should be addressed.
E-mail: choyj@kaeri.re.kr
‡This work was presented at the 7th China-Korea Workshop on Clean Energy Technology held at Taiyuan, Shanxi, China, June 26-28, 2008.

in diameter and 0.653 m in height as shown in Fig. 1. The column is made from Inconnel 600 materials. Corrosion tests have shown that Inconnel 600 has an acceptable corrosion rate in sodium carbonate at operating conditions. Sodium carbonate (melting point: 850 °C) and air were used as the liquid and gas phase, respectively. Oxidizing air is fed into the molten carbonate salts bed through a 0.013 m inner diameter vertical single tube. The column is heated by the surrounding ceramic three-zone heaters. The superficial gas velocity of the gas phase varied from 0.05-0.23 m/s, and the temperature of the molten salt bed ranged from 870-970 °C. The physical properties of the molten sodium carbonate with the temperature are given in Table 1.

The gas holdup was evaluated from the pressure drop measurement method using a differential pressure transducer. To measure the differential pressure drop, ΔP, two stainless steel tube tubes (SUS 316) were installed vertically in the molten salt bed. The vertical distance between the pressure measuring points, ΔL was 0.3 m. The out put voltage-time signals form the differential pressure transducer, corresponding to the pressure-time signal, were processed with the aid of a data acquisition system. The differential pressure signals were sampled at a rate of 200 Hz for 20 sec, yielding 4,000 data points. This combination of the sampling rate and time can detect the full spectrum of the hydrodynamic signals in multiphase flow system [9]. The gas phase holdup (ε_G) was calculated from the following equation.

$$\varepsilon_G = \frac{\frac{\Delta P}{\Delta L g} - \rho_L}{\rho_G - \rho_L} \quad (1)$$

Table 1. Physical properties of the molten sodium carbonate with the temperature

Temperature (°C)	Density (kg/m^3)	Viscosity (Pa·s)	Surface tension (dyne/cm)
870	2,476.62	4.1×10^{-3}	211
900	2,476.54	3.0×10^{-3}	210
930	2,476.46	2.2×10^{-3}	208
970	2,476.35	1.6×10^{-3}	206

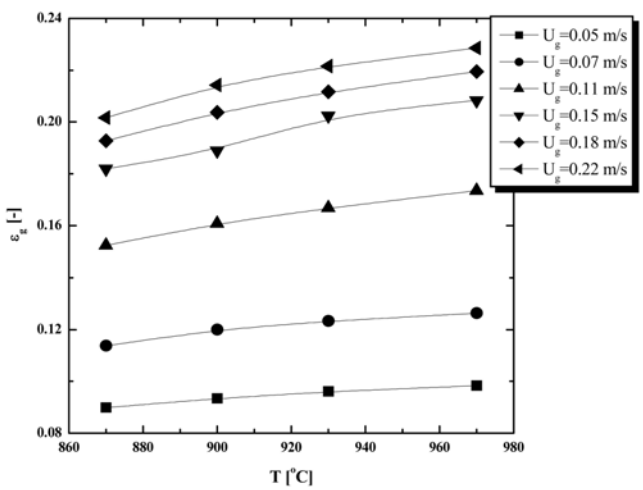

Fig. 2. Effects of the molten salt temperature on the gas holdup.

where, ρ_L and ρ_G are the density of the liquid (molten carbonate salt) and the gas (air), respectively.

RESULTS AND DISCUSSION

Effects of the molten sodium carbonate salt temperature on the gas holdup can be seen in Fig. 2, with a variation of the superficial gas velocity. In this figure, the gas holdup increases with an increasing gas velocity and temperature. Where, when the gas velocity exceeds 0.15 m/s, the increasing trend of the gas holdup is changed. The change of the increasing trend with the gas velocity may be due to the flow regime transition [10]. The increasing trend of the gas holdup with the temperature in a molten salt oxidation reactor

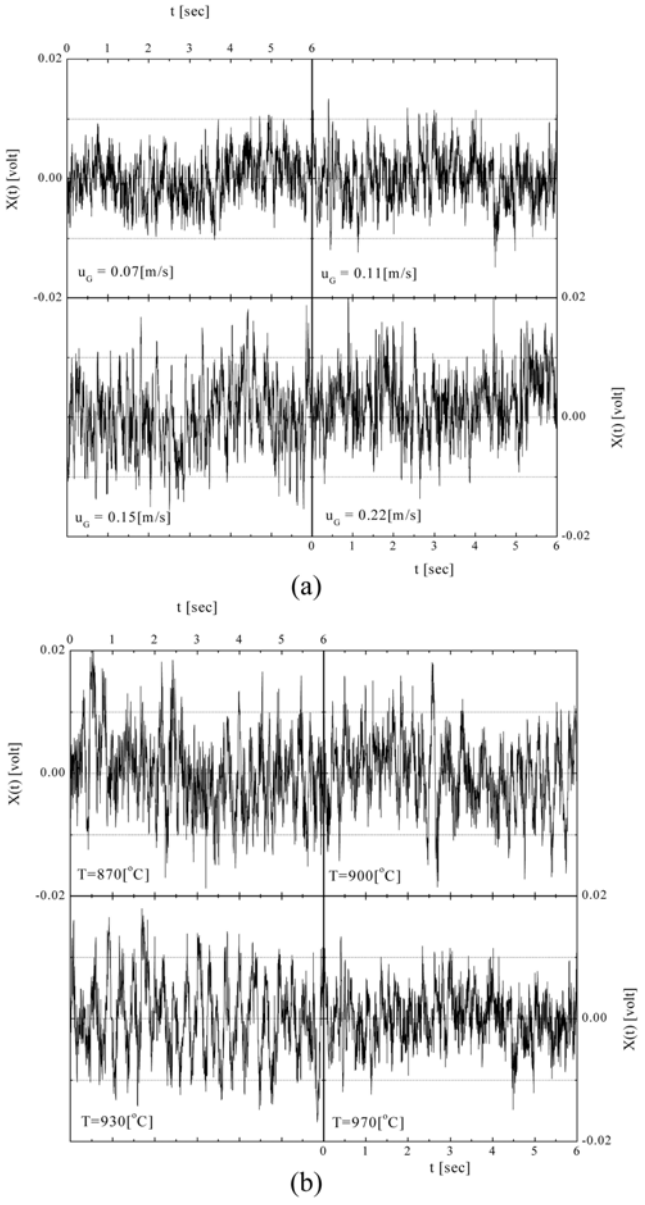

Fig. 3. Typical example of the differential pressure fluctuations with the air velocity (a) and the molten salt temperature (b) at a constant temperature (970 °C) and air velocity (0.11 m/s), respectively.

is in agreement with the observations of several researchers in a bubble column. Lin et al. [11] noted that the increasing trend of the gas holdup with the temperature is due to the dominant rule of the associated reduction in the liquid viscosity and the surface tension, which leads to a smaller average bubble size and a narrower bubble-size distribution, and they also noted that the associated increase in the gas density plays a secondary role. Pohorecki et al. [12] suggested that the influence of the surface tension of the gas holdup is greater than that of the liquid viscosity. The surface tension and viscosity of the molten sodium carbonate salt is decreased with an increasing temperature in the molten salt oxidation process. So, it is anticipated that the increasing trend of the gas holdup with the temperature is due to the decreasing tendency of the surface tension and the viscosity of the molten sodium carbonate salt with the temperature.

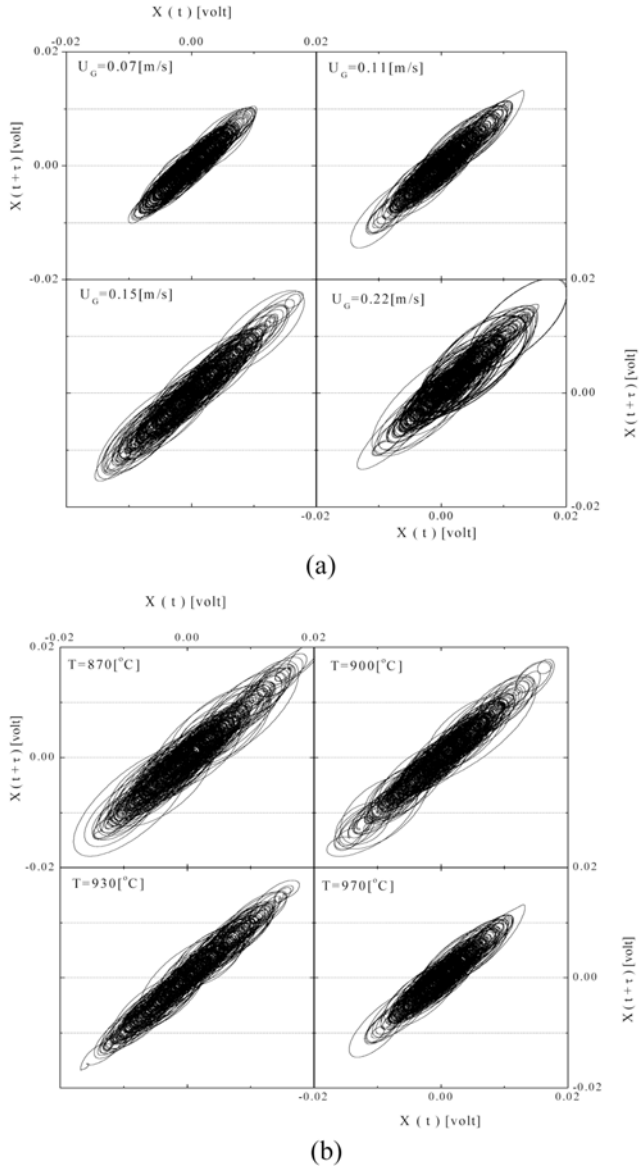

Fig. 4. Phase space portraits of the differential pressure fluctuations with the air velocity (a) and the molten salt temperature (b) at a constant temperature (970 °C) and air velocity (0.11 m/s), respectively.

The flow characteristics of a multi phase flow system can be described more conveniently by phase space portraits from a differential pressure fluctuation [13,14]. Typical example of a differential pressure fluctuation in a molten salt oxidation reactor can be seen in Fig. 3. As shown in Fig. 3, the differential pressure fluctuations depend on the air flow rate and the molten salt temperature, i.e. the pressure fluctuation signal is more complex with an increasing air flow rate but when the air flow rate exceeds 0.15 m/s, it shows a nearly similar complexity. With an increasing molten salt temperature, the amplitude of the pressure fluctuations is decreased, which is identical to the gas holdup tendency. These differential pressure fluctuations can be utilized more conveniently to visualize the complex behavior by means of phase space portraits in a reconstructed trajectory. Examples of the phase space portraits from the differential pressure fluctuation can be seen in Fig. 4, where the optimum time lag, for the construction of the phase space portraits is chosen when the mutual information function attains its first minimum value [15]. As shown in Fig. 4, the trajectory of the phase space portraits becomes more scattered with an increasing air velocity. The increase of the air flow rate results in an increase of the bubble size which eventually results in a less uniform bubble size distribution, so, the loop of the phase space portraits tends to be scattered with an increasing air flow rate. With an increasing molten salt temperature, the phase space portrait becomes less scattered and complex, i.e. more and more stabilized, which means that in the molten salt oxidation process, the flow is stabilized more with an increasing molten salt temperature.

To express the flow characteristics more easily and quantitatively, the Shannon entropy has been employed. The Shannon entropy can be utilized to express the degree of uncertainty in being able to predict the output of a probabilistic event [16]. That is to say, if one predicts the outcome exactly before it happens, the probability will be a maximum value and, as a result, the Shannon entropy will be a minimum value. If one can absolutely predict the outcome of an

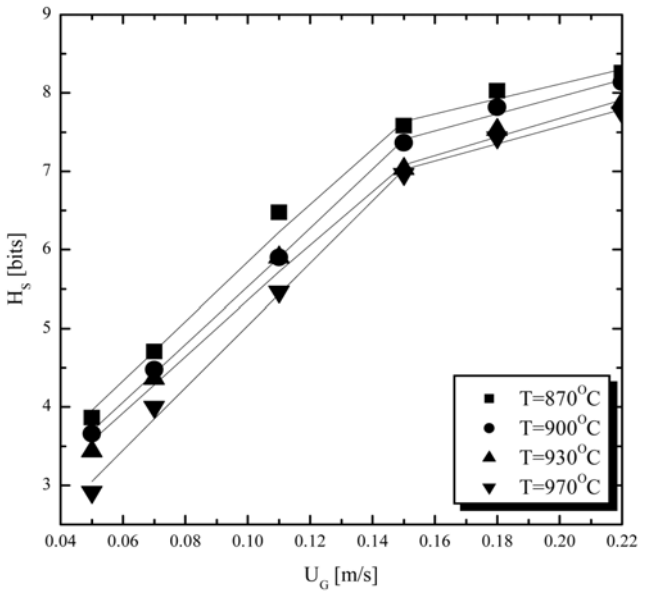

Fig. 5. Effects of the gas velocity and temperature on the Shannon Entropy in a molten salt oxidation reactor.

event, the Shannon entropy will be zero. If the data has r, the number of possible outcomes whose probabilities are P_1, P_2, P_r, then the Shannon entropy can be obtained by

$$H_S = \sum_{i=1}^{r} P_i \ln \frac{1}{P_i} \quad (2)$$

Effects of the gas velocity and the molten salt temperature on the Shennon entropy (Hs) can be seen in Fig. 5. In this figure, the value of the Shannon entropy increased with an increasing gas velocity, but decreased with an increasing temperature. Similar to the case of the gas holdup, the increasing trend of the Shannon entropy is changed at 0.15 m/s of a gas velocity. In the gas-liquid vertical up-flow system, the flow regime, with an increase in the gas velocity, gradually develops to a homogeneous flow and a heterogeneous flow. The heterogeneous flow is divided into three flow regimes with the gas velocity; bubble-slug, churn-turbulent or slug flow [17]. The prevailing regime mainly depends on the gas velocity, liquid properties and gas distributor [18]. In the case of the molten salt oxidation reactor system, the density of the liquid phase (molten sodium carbonate) is greater than the water, and the gas is dispersed to the molten salt bed through a single point sparging tube which produces a non-uniform gas distribution. So, it is anticipated that the flow regime develops from a bubble-slug to a slug flow with the gas velocity. A further increase of the gas velocity above 0.15 m/s produces a plug-like flow behavior. Since the Shannon entropy expresses the degree of uncertainty in the multi phase flow system, the decrease of the Shannon entropy with an increasing molten carbonate salt temperature means that the air-molten salt two phase flow system is stabilized more.

The drift-flux model has been used frequently for the fitting of gas holdup data [19]. Based on the drift-flux model, the gas holdup, in a liquid-batch system, is fitted in the form of Eq. (3).

$$\varepsilon_G = \frac{U_G}{C_o U_G + C_1} \quad (3)$$

where, C_o is a constant measure of the interaction of the void and velocity distribution, and C_1 is the weighted average drift velocity accounting for the local slip. C_1 is often taken as the rise velocity of a bubble in an infinite medium. Fig. 6(a) shows a typical example of a fitting result of the model equations, and the comparison between the experimental and correlated values of the gas holdup including the resulting value for the best fit of Eq. (3) is shown in Fig. 6(b). As can be seen, the best correlation of the gas holdup is accomplished by the drift-flux model for in the molten salt oxidation reactor.

In the conditions of 0.05-0.22 m/s of a gas velocity and 870-970 °C of a molten salt temperature, the values of the Shannon entropy have been correlated with the operating variables as Eq. (4) and the dimensionless experimental variables as Eq. (5) with correlation coefficients of 0.962 and 0.971, respectively (Fig. 7).

$$H_S = 1.3\times10^{5} U_G^{0.593} T^{-1.281} \quad (4)$$

$$H_S = 19.051\left(\frac{\mu_L^4 g}{\rho_L \sigma_L^3}\right) - 0.109\left(\frac{U_G \mu_L}{\rho_L}\right) 0.592 \quad (5)$$

Eq. (5) covers the range of variables, $3.04\times10^{-12} \le \mu_L^4 g/\rho_L \sigma_L^3 \le 1.18\times10^{-10}$, $1.71\times10^{-3} \le (U_G)\mu_L/\rho_L \le 1.30\times10^{-2}$. These correlation equations can be effectively utilized to predict the optimum operating condition, and for a scale-up of the molten salt oxidation process

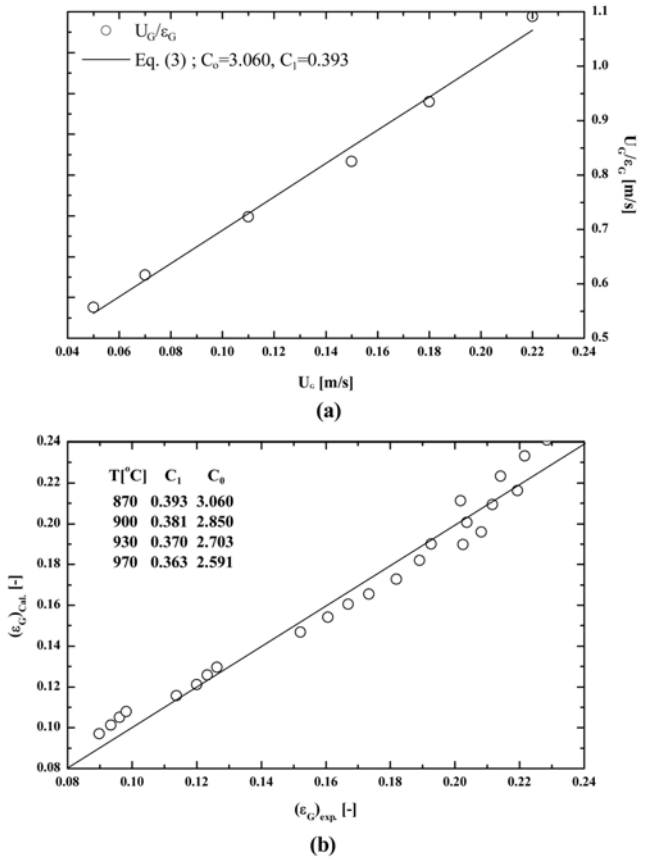

Fig. 6. Fitting result of the model equations (a), and the comparison between the experimental and correlated value of the gas holdup (b).

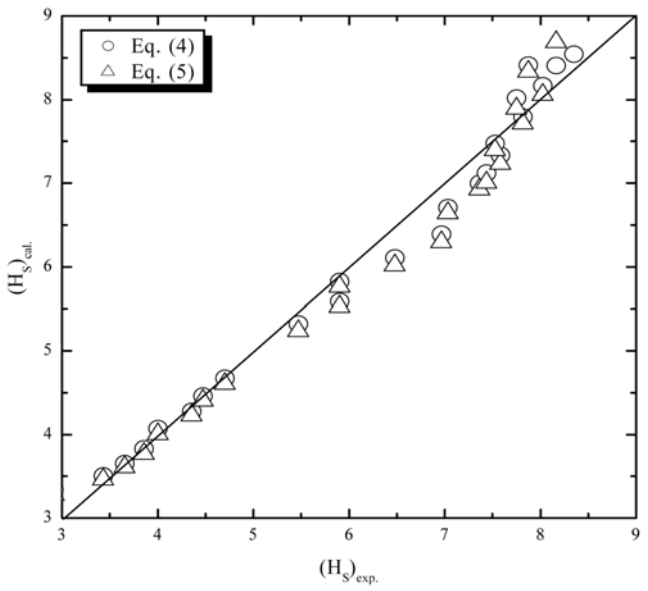

Fig. 7. Comparison of the experimentally obtained and calculated values of the Shannon entropy in a molten salt oxidation reactor.

for the best operation.

CONCLUSION

In the molten salt oxidation reactor, the gas phase holdup increases with an increase of the gas velocity and the molten sodium carbonate salt temperature. But the increasing trend of the gas holdup shows a different trend at gas velocities above 0.15 m/s under all the experimental temperature conditions, which may due to the flow regime transition. The highly complicated and nonlinear air-molten salt two phase flow systems in the molten salt oxidation reactor have been characterized successfully by a stochastic analysis of the differential pressure fluctuations: phase space portraits, Shannon entropy. The experimentally obtained values of the gas phase holdup and the Shannon entropy are correlated well by the drift-flux model and operating variables, respectively. These results may be useful for the design and operation of a molten salt oxidation process.

ACKNOWLEDGMENTS

This work has been performed under the Nuclear R&D program by Ministry of Education, Science and Technology.

NOMENCLATURE

C_0, C_1 : drift flux parameters in Eq. (3) [-]
g : gravity acceleration [m/s^2]
Hs : Shannon entropy [bits]
ΔL : vertical distance between pressure measuring point [m]
ΔP : differential pressure drop [atm]
r : number of possible outcomes in Eq. (2) [bit]
T : molten carbonate salt temperature [°C]
U_G : superficial gas velocity [m/s]
X(t) : time series of pressure fluctuations [volt]

Greek Letters

ε_G : gas phase holdup [-]
μ_L : liquid viscosity [Pa·s]
τ : time delay [sec]
ρ_L : liquid density [kg/m^3]
σ_L : liquid surface tension [dyne/cm]

REFERENCES

1. W. D. Deckwer, R. Burckhart and G. Zoll, *Chem. Eng. Sci*., **29**, 2177 (1974).
2. Y. Kang, J. S. Shim, M. H. Ko and S. D. Kim, *Korean J. Chem. Eng*., **13**, 317 (1996).
3. S. J. Kim, Y. J. Cho, C. G. Lee, Y. Kang and S. D. Kim, *Korean J. Chem. Eng*., **19**, 175 (2002).
4. J. H. Bell, P. A. Hass and J. C. Rudolph, *Sep. Sci. Technol*., **30**, 1755 (1995).
5. P. C. Hsu, K. G. Foster, T. D. Ford, P. H. Wallman, E. Watkins, C. O. Pruneda and M. G. Adamson, *Waste Management*, **20**, 363 (2000).
6. M. G. Adamson, P. C. Hsu, D. L. Hipple, K. G. Foster, R. W. Hopper and T. D. Ford, in G. E. Marcelle (Ed.), France, 1 (1998).
7. C. O. Pruned, B. E. Watkins and R. S. Upadhye, JANNAF Propulsion and Subcommittee Joint Meeting, December, FL (1995).
8. M. Alam and S. Kamath, *Environ. Sci. Technol*., **32**, 3986 (1998).
9. C. Vial, S. Poncin, G. Wild and N. Midoux, *Chem. Eng. Proc*., **40**, 135 (2001).
10. K. J. Woo, Y. J. Cho, K. I. Kim, Y. Kang and S. D. Kim, *HWAHAK KONGHAK*, **36**, 937 (1998).
11. T. J. Lin, K. Tsuchiya and L. S. Fan, *AIChE J*., **44**, 545 (1998).
12. R. Pohorecki, W. Moniuk, A. Zdrojkowski and P. Bielski, *Chem. Eng. Sci*., **56**, 1167 (2001).
13. Y. J. Cho, P. S. Song, S. H. Kim, Y. Kang and S. D. Kim, *J. Chem. Eng. of Japan*, **34**, 254 (2001).
14. Y. J. Cho, K. J. Woo, Y. Kang and S. D. Kim, *Chem. Eng. Pro*., **41**, 699 (2002).
15. L. T. Fan, Y. Kang, M. Yashima and D. Neogi, *Chem. Eng. Comm*., **135**, 147 (1995).
16. Y. Kang, K. J. Woo, M. H. Ko, Y. J. Cho and S. D. Kim, *Korean J. Chem. Eng*., **16**, 784 (1999).
17. L. S. Fan, Butterworths, MA (1989).
18. Y. Kang and S. D. Kim, *Ind. Eng. Chem. Process Des. Dev*., **25**, 717 (1986).
19. J. Zahradnik, M. Fialova, M. Ruzicka, J. Drahos, F. Kastanek and N. H. Thomas, *Chem. Eng. Sci*., **52**, 3811 (1997).